J|A|C|S
ARTICLES
Published on Web 03/23/2007

Base-Dependent Electron Photodetachment from Negatively Charged DNA Strands upon 260-nm Laser Irradiation

Valérie Gabelica,*,† Frédéric Rosu,† Thibault Tabarin,‡ Catherine Kinet,† Rodolphe Antoine,‡ Michel Broyer,‡ Edwin De Pauw,† and Philippe Dugourd*,‡

Contribution from the Laboratoire de Spectrométrie de Masse, Université de Liège, Institut de Chimie Bat B6c, B-4000 Liège, Belgium and the Université Lyon 1, CNRS, LASIM UMR 5579, bât. A. Kastler, 43 Bd du 11 Novembre 1918, F-69622 Villeurbanne, France

Received December 5, 2006; E-mail: v.gabelica@ulg.ac.be; dugourd@lasim.univ-lyon1.fr

Abstract: DNA multiply charged anions stored in a quadrupole ion trap undergo one-photon electron ejection (oxidation) when subjected to laser irradiation at 260 nm (4.77 eV). Electron photodetachment is likely a fast process, given that photodetachment is able to compete with internal conversion or radiative relaxation to the ground state. The DNA $[6\text{-mer}]^{3-}$ ions studied here show a marked sequence dependence of electron photodetachment yield. Remarkably, the photodetachment yield ($dG_6 > dA_6 > dC_6 > dT_6$) is inversely correlated with the base ionization potentials (G < A < C < T). Sequences with guanine runs show increased photodetachment yield as the number of guanine increases, in line with the fact that positive holes are the most stable in guanine runs. This correlation between photodetachment yield and the stability of the base radical may be explained by tunneling of the electron through the repulsive Coulomb barrier. Theoretical calculations on dinucleotide monophosphates show that the HOMO and HOMO-1 orbitals are localized on the bases. The wavelength dependence of electron detachment yield was studied for dG_6^{3-}. Maximum electron photodetachment is observed in the wavelength range corresponding to base absorption (260−270 nm). This demonstrates the feasibility of gas-phase UV spectroscopy on large DNA anions. The calculations and the wavelength dependence suggest that the electron photodetachment is initiated at the bases and not at the phosphates. This also indicates that, although direct photodetachment could also occur, autodetachment from excited states, presumably corresponding to base excitation, is the dominant process at 260 nm. Excited-state dynamics of large DNA strands still remains largely unexplored, and photo-oxidation studies on trapped DNA multiply charged anions can help in bridging the gap between gas-phase studies on isolated bases or base pairs and solution-phase studies on full DNA strands.

Introduction

The key issue for understanding DNA photostability upon UV irradiation is the nature of the relaxation processes that convert the electronic energy susceptible of causing photochemical reactions into less harmful vibrational energy. Nucleic acids are highly vulnerable in the UVC range of the solar spectrum (<290 nm), where direct $\pi\pi \rightarrow \pi\pi^*$ excitation of the bases occurs. Numerous theoretical[1−3] and experimental[4−6] studies on excited-state relaxation dynamics of isolated bases and base pairs have highlighted very efficient pathways that relax electronic energy to the ground state in less than a picosecond.[7−9] This fast conversion has been thought to explain the good photostability of DNA bases that were evolutionary selected as the carriers of genetic information.[10−12] However, the picture gets much more complex when it comes to excited-state dynamics of whole DNA strands. The presence of longer-lived (up to nanoseconds)[13] excited states was revealed in time-resolved spectroscopy studies on DNA single strands and double strands in solution. The multiple decay pathways and long-lived intermediates encountered in DNA strands compared to isolated nucleobases reveal the high complexity of relaxation mechanisms in these more biologically relevant models.[14−18] The

† Université de Liège.
‡ Université Lyon 1 and CNRS.

(1) Sobolewski, A. L.; Domcke, W. *Eur. Phys. J. D* **2002**, *20*, 369−374.
(2) Shukla, M. K.; Leszczynski, J. *J. Comput. Chem.* **2004**, *25*, 768−778.
(3) Perun, S.; Sobolewski, A. L.; Domcke, W. *J. Am. Chem. Soc.* **2005**, *127*, 6257−6265.
(4) Ullrich, S.; Schultz, T.; Zgierski, M. Z.; Stolow, A. *J. Am. Chem. Soc.* **2004**, *126*, 2262−2263.
(5) Ritze, H. H.; Lippert, H.; Samoylova, E.; Smith, V. R.; Hertel, I. V.; Radloff, W.; Schultz, T. *J. Chem. Phys.* **2005**, *122*, 224320.
(6) Ullrich, S.; Schultz, T.; Zgierski, M. Z.; Stolow, A. *Phys. Chem. Chem. Phys.* **2004**, *6*, 2796−2801.
(7) Samoylova, E.; Lippert, H.; Ullrich, S.; Hertel, I. V.; Radloff, W.; Schultz, T. *J. Am. Chem. Soc.* **2005**, *127*, 1782−1786.
(8) Crespo-Hernandez, C. E.; Cohen, B.; Hare, P. M.; Kohler, B. *Chem. Rev.* **2004**, *104*, 1977−2019.
(9) Hare, P. M.; Crespo-Hernandez, C. E.; Kohler, B. *Proc. Natl. Acad. Sci. U.S.A.* **2007**, *104*, 435−440.
(10) Satzger, H.; Townsend, D.; Zgierski, M. Z.; Patchkovskii, S.; Ullrich, S.; Stolow, A. *Proc. Natl. Acad. Sci. U.S A.* **2006**, *103*, 10196−10201.
(11) Sobolewski, A. L.; Domcke, W.; Hattig, C. *Proc. Natl. Acad. Sci. U.S.A.* **2005**, *102*, 17903−17906.
(12) Schultz, T.; Samoylova, E.; Radloff, W.; Hertel, I. V.; Sobolewski, A. L.; Domcke, W. *Science* **2004**, *306*, 1765−1768.
(13) Plessow, R.; Brockhinke, A.; Eimer, W.; Kohse-Hoinghaus, K. *J. Phys. Chem. B* **2000**, *104*, 3695−3704.
(14) Markovitsi, D.; Onidas, D.; Gustavsson, T.; Talbot, F.; Lazzarotto, E. *J. Am. Chem. Soc.* **2005**, *127*, 17130−17131.
(15) Crespo-Hernandez, C. E.; Cohen, B.; Kohler, B. *Nature* **2005**, *436*, 1141−1144.
(16) Markovitsi, D.; Talbot, F.; Gustavsson, T.; Onidas, D.; Lazzarotto, E.; Marguet, S. *Nature* **2006**, *441*, E7.

10.1021/ja068440z CCC: $37.00

interpretation of the solution-phase results is also complicated by the intrinsic heterogeneity of the oligonucleotide models exposed to UV irradiation, which can be either conformational heterogeneity or chemical heterogeneity in the case of photo-induced reactions in the sample during the experiment.[19]

Isolated DNA strands in the gas phase are good models to bridge the gap between molecular beam studies on isolated bases and solution-phase studies on full-length DNA. While molecular beams produce neutral molecules, electrospray produces ions directly from the solution by protonation/deprotonation reactions or cation/anion addition.[20−22] In the case of DNA strands, electrospray produces multiply charged anions by desolvation of the DNA anions that were present in solution. Those negative ions are close to the solution model in the sense that they are closed-shell ions, the multiple charges coming from deprotonation. However, working with anions causes some methodological difficulties. When studying neutral molecules or aggregates, the electronic transitions can be studied with resonant two-photon experiments, the second photon leading to the ionization of the molecule, but when the molecules under study are already ionized, other ways of studying electronically excited states must be used, for example, via the detection of ion fragmentation. In the field of mass spectrometry, there is currently a renewed interest in photodissociation of electrosprayed ions, pioneered by McLafferty and co-workers,[23,24] as a new fragmentation technique for peptides and proteins that leads to new fragmentation channels.[25,26] In the field of gas-phase spectroscopy, wavelength-resolved photodissociation experiments of electrosprayed ions (usually cations obtained by protonation) have now been reported by several groups, either in the UV−vis range[27−35] or in the infrared.[36−42]

With the aim of studying electronic excitation of multiply charged DNA anions (single strands and double helices), we started an exploration of the fragmentation pathways by UV irradiation between 220 and 290 nm (corresponding to absorption of the nucleic bases) and found that the major observable reaction was electron detachment.[43] Our first study on different DNA single strands and double strands suggested that the electron photodetachment yield was directly dependent on the number of guanines in the strand, and we initially postulated that guanines were mandatory for electron photodetachment to occur.[43] In the present paper, we show that there is a strong dependence of electron photodetachment yield on the base sequence and that electron detachment yield is inversely correlated to the base ionization potentials. We will discuss the possible electron photodetachment mechanisms, the competition between electron detachment and other fragmentation pathways, and the implications for future DNA photophysics studies.

Experimental Section

Sample Preparation. All oligonucleotides used in this study were provided by Eurogentec (Liege, Belgium), with Oligold quality. The oligonucleotides were solubilized in doubly distilled water to obtain stock solutions with single-strand concentration of 200 μM. Solutions injected in the mass spectrometers were diluted to 25 μM, in 50/50 (v:v) water/methanol.

Electrospray Mass Spectrometry and Laser Irradiation of Trapped Ions. The experiments were performed on a commercial LCQ Duo quadrupole ion trap mass spectrometer (ThermoFinnigan, San Jose, CA) coupled to a Panther OPO laser pumped by a 355-nm Nd:YAG PowerLite 8000 (5-ns pulse width, 20 Hz repetition rate). Frequency doubling allows scanning in the range 215−300 nm. The standard electrospray source was operated as described previously.[43] The vacuum chamber and the central ring electrode of the mass spectrometer were modified to allow the injection of UV and visible lights.[44] A fiber optics glued to the ion trap opposite the incoming beam was used for laser alignment, ensuring reproducible overlap between the laser beam and the ion cloud. An electromechanical shutter triggered on the radio-frequency (RF) signal of the ion trap synchronizes the laser irradiation with the tandem mass spectrometry (MS/MS) events conducted in the ion trap. To perform laser irradiation for a given number of laser pulses, we add an MS^n step with activation amplitude of 0%, during which the shutter is open. Therefore, at 20 Hz, 50-ms activation time corresponds to one laser pulse, 100 ms corresponds to two laser pulses, and so forth. The laser power was controlled using a half-wave plate and a polarizer and was monitored with a power meter located just before the injection in the ion trap.

Theoretical Calculations. Conformer distributions of the deprotonated dinucleotide monophosphates were obtained from a Monte Carlo conformational search using Spartan O4 (Wavefunction Inc.) at the semiempirical AM1 level. For each dinucleotide, two or three significantly different lowest energy conformers were further optimized at the HF/6-31+G(d, p) level. Correlation energy was taken into account

(17) Crespo-Hernandez, C. E.; Cohen, B.; Kohler, B. *Nature* **2006**, *441*, E8.
(18) Kwok, W. M.; Ma, C.; Phillips, D. L. *J. Am. Chem. Soc.* **2006**, *128*, 11894−11905.
(19) Markovitsi, D.; Onidas, D.; Talbot, F.; Marguet, S.; Gustavsson, T.; Lazzarotto, E. *J. Photochem. Photobiol., A* **2006**, *183*, 1−8.
(20) Fenn, J. B.; Mann, M.; Meng, C. K.; Wong, S. F.; Whitehouse, C. M. *Science* **1989**, *246*, 64−71.
(21) Fenn, J. B.; Mann, M.; Meng, C. K.; Wong, S. F. *Mass Spectrom. Rev.* **1990**, *9*, 37−70.
(22) Cech, N. B.; Enke, C. G. *Mass Spectrom. Rev.* **2001**, *20*, 362−387.
(23) Williams, E. R.; Furlong, J. J. P.; McLafferty, F. W. *J. Am. Soc. Mass Spectrom.* **1990**, *1*, 288−294.
(24) Guan, Z.; Kelleher, N. L.; O'Connor, P. B.; Aaserud, D. J.; Little, D. P.; McLafferty, F. W. *Int. J. Mass Spectrom. Ion Processes* **1996**, *157−158*, 357−364.
(25) Kim, T. Y.; Thompson, M. S.; Reilly, J. P. *Rapid Commun. Mass Spectrom.* **2005**, *19*, 1657−1665.
(26) Moon, J. H.; Yoon, S. H.; Kim, M. S. *Rapid Commun. Mass Spectrom.* **2005**, *19*, 3248−3252.
(27) Nolting, D.; Marian, C.; Weinkauf, R. *Phys. Chem. Chem. Phys.* **2004**, *6*, 2633−2640.
(28) Marian, C.; Nolting, D.; Weinkauf, R. *Phys. Chem. Chem. Phys.* **2005**, *7*, 3306−3316.
(29) Andersen, L. H.; Heber, O.; Zajfman, D. *J. Phys. B: At. Mol. Opt. Phys.* **2004**, *37*, R57−R88.
(30) Nielsen, S. B.; Lapierre, A.; Andersen, J. U.; Pedersen, U. V.; Tomita, S.; Andersen, L. H. *Phys. Rev. Lett.* **2001**, *8722* (22), 228102.
(31) Andersen, L. H.; Lapierre, A.; Nielsen, S. B.; Nielsen, I. B.; Pedersen, S. U.; Pedersen, U. V.; Tomita, S. *Eur. Phys. J. D* **2002**, *20*, 597−600.
(32) Talbot, F. O.; Tabarin, T.; Antoine, R.; Broyer, M.; Dugourd, P. *J. Chem. Phys.* **2005**, *122* (7), 074310.
(33) Tabarin, T.; Antoine, R.; Broyer, M.; Dugourd, P. *Rapid Commun. Mass Spectrom.* **2005**, *19*, 2883−2892.
(34) Kang, H.; Jouvet, C.; donder-Lardeux, C.; Martrenchard, S.; Gregoire, G.; Desfrancois, C.; Schermann, J. P.; Barat, M.; Fayeton, J. A. *Phys. Chem. Chem. Phys.* **2005**, *7* (2), 394−398.
(35) Boyarkin, O. V.; Mercier, S. R.; Kamariotis, A.; Rizzo, T. R. *J. Am. Chem. Soc.* **2006**, *128*, 2816−2817.
(36) Oomens, J.; Polfer, N.; Moore, D. T.; van der Meer, L.; Marshall, A. G.; Eyler, J. R.; Meijer, G.; von Helden, G. *Phys. Chem. Chem. Phys.* **2005**, *7*, 1345−1348.
(37) Oh, H. B.; Lin, C.; Hwang, H. Y.; Zhai, H. L.; Breuker, K.; Zabrouskov, V.; Carpenter, B. K.; McLafferty, F. W. *J. Am. Chem. Soc.* **2005**, *127*, 4076−4083.
(38) Polfer, N. C.; Valle, J. J.; Moore, D. T.; Oomens, J.; Eyler, J. R.; Bendiak, B. *Anal. Chem.* **2006**, *78*, 670−679.
(39) Simon, A.; Jones, W.; Ortega, J. M.; Boissel, P.; Lemaire, J.; Maitre, P. *J. Am. Chem. Soc.* **2004**, *126*, 11666−11674.
(40) Polfer, N. C.; Oomens, J.; Dunbar, R. C. *Phys. Chem. Chem. Phys.* **2006**, *8*, 2744−2751.
(41) Polfer, N. C.; Paizs, B.; Snoek, L. C.; Compagnon, I.; Suhai, S.; Meijer, G.; von Helden, G.; Oomens, J. *J. Am. Chem. Soc.* **2005**, *127*, 8571−8579.
(42) Kamariotis, A.; Boyarkin, O. V.; Mercier, S. R.; Beck, R. D.; Bush, M. F.; Williams, E. R.; Rizzo, T. R. *J. Am. Chem. Soc.* **2006**, *128*, 905−916.
(43) Gabelica, V.; Tabarin, T.; Antoine, R.; Rosu, F.; Compagnon, I.; Broyer, M.; De Pauw, E.; Dugourd, P. *Anal. Chem.* **2006**, *78*, 6564−6572.
(44) Dugourd, P.; Antoine, R.; Broyer, M.; Talbot, F. O. International patent WO 2006064132, 2006.

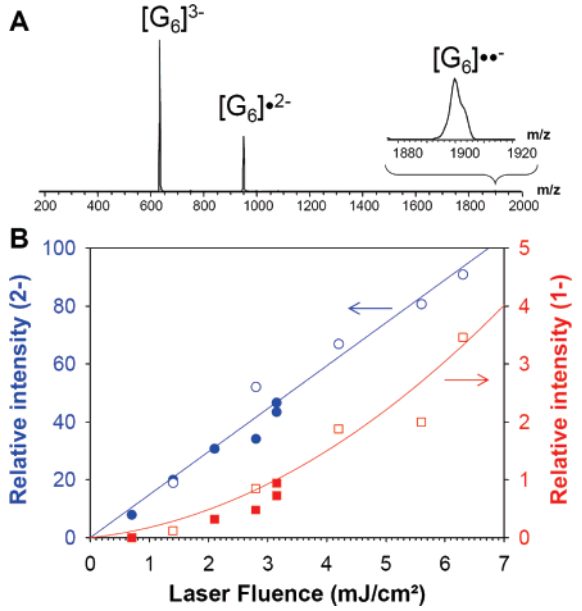

Figure 1. (A) Photodetachment mass spectrum of dG_6^{3-} under one laser pulse at 260 nm at 3.15 mJ/cm^2. The inset shows a zoom on the peak corresponding to a double-electron detachment. (B) Relative intensities of $dG_6^{\bullet 2-}$ (blue, left scale) and $dG_6^{\bullet\bullet 1-}$ (red, right scale) produced by laser irradiation of dG_6^{3-} as a function of the total laser fluence. One-pulse data are represented in full symbols while two-pulse data are represented in open symbols.

by performing single-point calculation at the MP2/6-31+G(d, p) level. The energies of the corresponding neutral radicals were obtained using restricted open-shell calculations (ROHF/6-31+G(d, p) and ROMP2/6-31+G(d, p)) to avoid spin contamination. All electronic structure calculations were performed using the PC GAMESS version 7.0 software.[45] The molecular orbitals were displayed using Chemcraft (http://www.chemcraftprog.com/) or MOLDEN (http://www.cmbi.ru.nl/molden/molden.html).

Results and Discussion

Electron Photodetachment from dG_6^{3-} Is a One-Photon Process at 260 nm. To get deeper insight into the electron photodetachment mechanism, an important issue is to establish the one-photon or multiphoton character of electron photodetachment observed when using 260-nm (4.77 eV) photons. We measure ion yields with the mass spectrometer (signal of radical ion resulting from electron photodetachment relative to the signal of the parent ion) but cannot determine quantum yields directly. The electron detachment ion yield depends on the electron detachment quantum yield and on the absorption efficiency. We therefore measured the electron detachment ion yield (or simply "electron detachment yield", as used throughout the forthcoming text) as a function of the laser power for dG_6^{3-} under one-pulse (50 ms) and two-pulse (100 ms) irradiation. dG_6^{3-} was chosen because of its high electron detachment yield, so that electron detachment was detectable even using a single-laser pulse at the reduced power obtained after the half-wave plate and the polarizer.

Figure 1A shows the mass spectrum obtained using a single-laser pulse at 3.15 mJ/cm^2. The inset shows the presence of double-electron photodetachment in the single-pulse experiments (5-ns laser pulse width). Figure 1B shows the plot of $I_{(\text{product})}$/

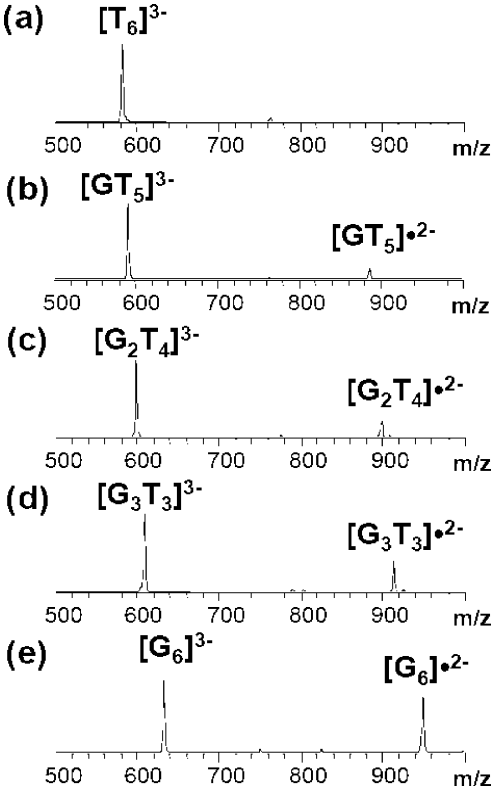

Figure 2. Electron photodetachment as a function of the guanine content: (a) $[dT_6]^{3-}$, (b) $[dGT_5]^{3-}$, (c) $[dG_2T_4]^{3-}$, (d) $d[G_3T_3]^{3-}$, and (e) $[dG_6]^{3-}$. All [6-mers]$^{3-}$ were isolated and subjected to a single 260-nm laser pulse, with identical laser focusing conditions and laser energy (fluence: 11.5 mJ/cm^2).

$I_{(\text{precursor})}$ as a function of the total laser energy for the first electron loss (3- →2-•). The linear increase indicates that the first electron photodetachment is a one-photon process. Red symbols correspond to the same plot for the double-electron loss (3- → 1-••). The quadratic increase indicates that this global reaction is a multiphoton process, most likely two-photon. Moreover, the fact that the one-pulse and two-pulse data (filled and open symbols, respectively) fall on the same lines suggests that the consecutive electron photodetachment steps are independent, that is, $dG_6^{\bullet\bullet 1-}$ is produced from $dG_6^{\bullet 2-}$ with equal efficiency either within the 5-ns single-pulse experiment or when a second pulse is applied after 50-ms cooling in the helium bath gas.

Base Dependence of Electron Photodetachment Yield. The second crucial point for the discussion of the electron photodetachment mechanism is the dependence on the nature of the base. Here, we studied DNA 6-mer single strands with various sequences. Figure 2 shows the mass spectra obtained after one laser pulse irradiation of the [6-mer]$^{3-}$ anions at 260 nm for the sequences G_nT_{6-n}. These spectra confirm the trend observed previously on DNA duplexes. The strand $[T_6]^{3-}$ does not encounter electron photodetachment.

The strong dependence of electron photodetachment yield is in line with a recent photoelectron study on electrosprayed ions that showed specific features at lower electron binding energy in $[dGMP-H]^-$ and in deprotonated polynucleotides (2/3-mers) containing at least one guanine.[46] On the basis of this observation

(45) Granovsky, A. A. PC Gamess v. 7.0. http://classic. chem. msu. su/gran/gamess/index.html (accessed 12/2006).

(46) Yang, X.; Wang, X. B.; Vorpagel, E. R.; Wang, L. S. *Proc. Natl. Acad. Sci. U.S.A.* **2004**, *101*, 17588−17592.

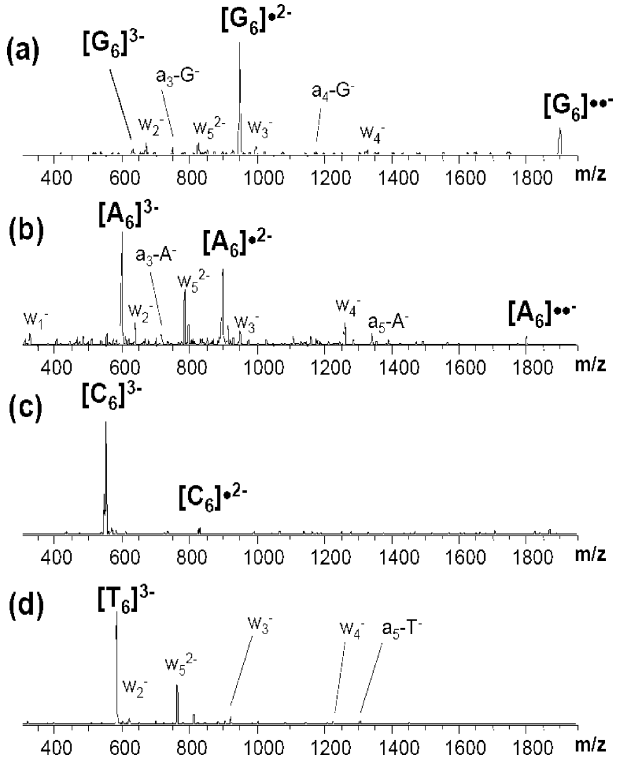

Figure 3. Electron photodetachment and secondary fragmentation as a function of the base: (a) $[dG_6]^{3-}$, (b) $[dA_6]^{3-}$, (c) $[dC_6]^{3-}$, and (d) $[dT_6]^{3-}$. All $[dB_6]^{3-}$ were isolated and subjected to 250-ms laser irradiation (five laser pulses) at 260 nm, with identical laser focusing conditions and laser energy (fluence per pulse: 11.5 mJ/cm^2).

and on density functional theory (DFT) calculations of the highest occupied molecular orbitals (HOMOs) of deoxynucleoside monophosphates, the authors concluded that guanine was the site of electron detachment. The strong guanine dependence of the electron photodetachment yield observed here is in line with the fact that guanine has the lowest ionization potential among all four DNA bases. Recently, several groups reported more advanced calculations of the vertical detachment energies of deoxynucleoside monophosphates, suggesting that the base could play a role in the lowest-energy oxidation in the cases of adenine and thymine as well.[47,48]

To try and detect electron detachment in non-guanine-containing DNA multiply charged strands, we performed experiments with more than one laser pulse. Figure 3 shows the results obtained for $[dG_6]^{3-}$, $[dA_6]^{3-}$, $[dC_6]^{3-}$, and $[dT_6]^{3-}$ using five laser pulses at 260 nm. Figure 3 shows that $[dA_6]^{3-}$, and to a lesser extent $[dC_6]^{3-}$, can also undergo electron photodetachment, while the only visible outcome of $[dT_6]^{3-}$ irradiation is fragmentation into the so-called a-base and w fragments, labeled according to Wu and McLuckey's nomenclature.[49] The competition between electron photodetachment and fragmentation will be discussed in more detail below. Guanine has by far the largest effect on the electron photodetachment yield, as shown in Figure 4 where the fraction of surviving parent ion is plotted as a function of the number of laser pulses (the slopes of the linear regressions are given in

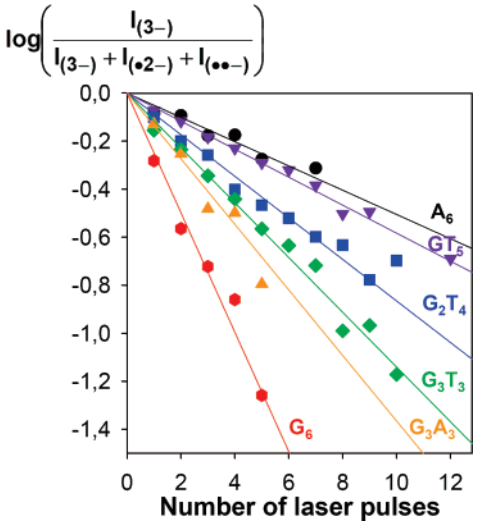

Figure 4. Dependence of electron photodetachment yield on the number of laser pulses as a function of the DNA sequence for [6-mers]$^{3-}$: dA_6 (black circles), dGT_5 (violet down triangles), dG_2T_4 (blue squares), dG_3T_3 (green diamonds), dG_3A_3 (orange up triangles), dG_6 (red hexagons).

Table 1. Slopes of the Linear Regressions Shown in Figure 4 and Molar Extinction Coefficients of Oligonucleotides in Solution at 260 nm

sequence	slope of linear regression	ϵ (L mol^{-1} cm^{-1}) @ 260 nm[50]
dT_6^{3-}	0	49 200
dC_6^{3-}	n.d.[a]	43 400
dA_6^{3-}	-0.050 ± 0.010	75 400
dGT_5^{3-}	-0.058 ± 0.002	52 400
$dG_2T_4^{3-}$	-0.087 ± 0.005	54 400
$dG_3T_3^{3-}$	-0.114 ± 0.006	56 400
$dG_3A_3^{3-}$	-0.137 ± 0.017	69 400
dG_6^{3-}	-0.249 ± 0.027	62 000

[a] Electron detachment is detected but is too small to allow quantification and linear regression.

Table 1). A single guanine in the sequence gives a larger electron detachment yield than six adenines.

We therefore investigated which base properties could explain the electron photodetachment yield ordering $dG_6^{3-} > dA_6^{3-} > dC_6^{3-} > dT_6^{3-}$. The efficiency of 260-nm photon absorption (oscillator strength) certainly has an influence on the photodetachment yield. This can be approximated by the molar extinction coefficient in solution at 260 nm,[50] which is given in Table 1 for all strands studied here. If photon absorption efficiency were the only base property controlling photodetachment yield, the ranking would be A > G > T > C. The base dependence can therefore not be explained by absorption efficiency.

We also included in the study the strand dG_3A_3 for comparison with dG_3T_3 to test whether only the number of guanines determines the efficiency of photodetachment after electronic excitation or whether all bases contributed to the process. However, we are not able to conclude whether the other bases also have an influence in the presence of guanines because the difference in photodetachment ion yield could be due in this case to the difference in absorption efficiency.

Alternatively, if we consider the potential correlation of electron photodetachment yield with the propensity of the base

(47) Rubio, M.; Roca-Sanjuan, D.; Merchan, M.; Serrano-Andres, L. *J. Phys. Chem. B* **2006**, *110*, 10234−10235.
(48) Zakjevskii, V. V.; King, S. J.; Dolgounitcheva, O.; Zakrzewski, V. G.; Ortiz, J. V. *J. Am. Chem. Soc.* **2006**, *128*, 13350−13351.
(49) Wu, J.; McLuckey, S. A. *Int. J. Mass Spectrom.* **2004**, *237*, 197−241.
(50) Fasman, G. D.; Sober, H. A. *Handbook of biochemistry and molecular biology: physical and chemical data, miscellaneous*; CRC Press: Cleveland, 1976.

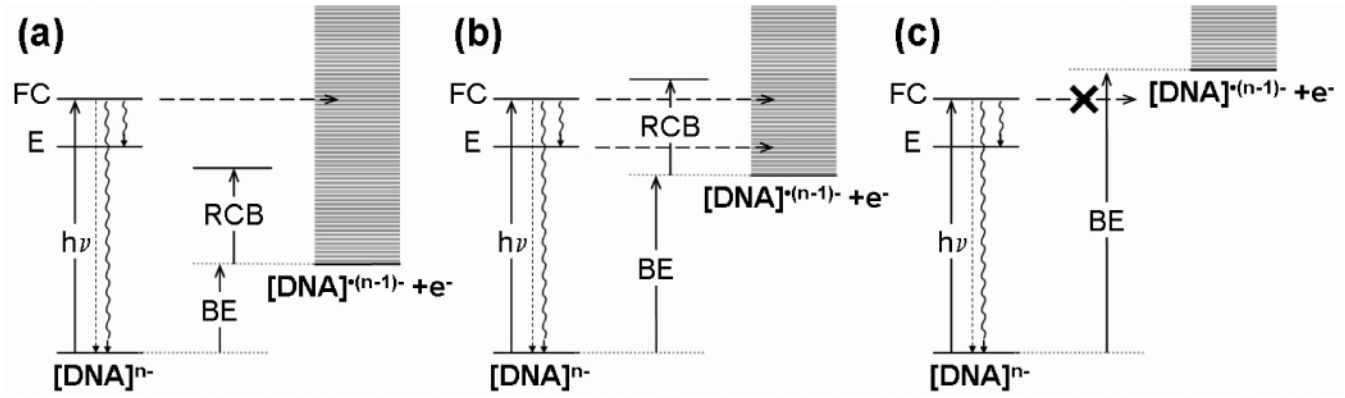

Figure 5. Scheme illustrating the fate of the Franck−Condon (FC) excited state and the possible electron photodetachment pathways. The electron binding energy (BE) is the energy difference between the closed-shell multianion $[DNA]^{n-}$ and the radical $[DNA]^{\bullet(n-1)-}$. The FC state can undergo radiative decay (short dashed arrows), internal conversion to the ground state (long wavy arrows), internal conversion to another electronic excited state E (short wavy arrows), or electron detachment (horizontal long dashed arrows). (a) If $h\nu > BE + RCB$, fast electron photodetachment from the FC state can occur. (b) If $BE < h\nu < BE + RCB$, electron autodetachment can occur by tunneling through the repulsive Coulomb barrier either from the FC state or from another excited state E. (c) If $h\nu < BE$, no photodetachment can occur. Direct electron photodetachment is not represented here but is possible if $h\nu > BE + RCB$.

to lose an electron, we should seek possible correlations with electron detachment energies of DNA bases or DNA strands, base ionization potentials (IP, energy difference between the neutral base and the base radical cation) if the electron is lost from a neutral base, or base electron affinities (EA, energy difference between the neutral base and the base radical anion) if the electron is lost from a base radical anion. The IP ranking of the neutral bases is G < A < C < T,[51,52] while the computed electron affinity ranking is T > C ≈ G > A for isolated bases and dT > dC > dG ≈ dA for deoxunucleosides.[53] The best correlation is therefore found with base ionization potentials, suggesting that the electron photodetachment yield is related to the ability of the neutral bases (the negative charges presumably being located on phosphate groups) to lose an electron. Yang et al.[46] recently determined adiabatic detachment energies (ADEs) for deprotonated mono-, di-, and trinucleotide, using photoelectron spectroscopy using 157-nm photons. The ADE ordering is $dG^- < dC^- < dT^- < dA^-$ for mononucleotides, $dGG^- < dCC^- < dAA^- < dTT^-$ for dinucleotides, and $dGGG^- < dAAA^- < dCCC^- < dTTT^-$ for trinucleotides. For 3-mers on, the electron detachment energies are therefore correlated to the base IPs. For the discussion of the electron photodetachment mechanism, it is tempting to postulate that all these correlations are not fortuitous.

On the Electron Photodetachment Mechanism. A one-photon oxidation at 260 nm ($h\nu = 4.77$ eV) suggests that electron binding energies (BE) of dB_6^{3-} are <4.77 eV (except perhaps for dT_6^{3-}, for which no photodetachment is observed). This is not surprising in the case of multiply charged anions because of the Coulomb repulsion. Negative electron binding energies are even possible as shown by a photoelectron spectroscopy study of dA_5^{4-}.[54] These charge states in the ground electronic state can nevertheless be stable on the time scale of the experiment because of the repulsive Coulomb barrier (RCB).[55,56] Direct electron photodetachment without transition via a Franck−Condon (FC) state of the closed-shell ion is possible if $h\nu > RCB + BE$. However, an argument in the favor of a major contribution of autodetachment of excited states is the wavelength dependence of electron detachment yield, which is maximum at wavelengths corresponding to base absorption (see ref 43 and discussion below).

The Franck−Condon (FC) excited states obtained by the initial photon absorption can evolve via the following pathways (Figure 5): internal conversion to the ground state or internal coupling to other excited states E (wavy arrows), radiative decay (dashed arrows) to the ground state, or electron detachment (horizontal dashed arrows). If $h\nu > RCB + BE$ (Figure 5a), electron detachment from the FC state can be very fast. If $BE < h\nu < RCB + BE$ (Figure 5b), electron detachment can proceed by tunneling from the FC state through the RCB. If $h\nu < BE$, no photodetachment can occur (Figure 5c). While some authors suggested that FC states are delocalized,[14,57] a recent study suggests that FC states are localized on a base[18] and that internal conversion to excimer-like states can occur within ~400 fs.[15,18] In the same way, this second excited state E can undergo internal conversion to ground state, radiative decay, electron autodetachment, conversion to another electronic state, and so forth.

Radiative decay cannot be detected in our experimental setup, but internal conversion to the ground state manifests itself by the formation of the a-base and w fragments, which are the typical fragments formed by collisional activation of deprotonated closed-shell oligodeoxynucleotides.[49] The presence of these fragments indicates that a fraction of the electronic energy can be converted into vibrational energy. Total internal conversion to the ground state should be efficient and fast, given the high density of states of these large ions. The very fast pathways demonstrated for isolated bases and base pairs are actually thought to be at the origin of the high photostability of DNA bases.[10−12] The fact that in most of our experiments electron photodetachment is able to compete with internal conversion is therefore a good indication that electron photodetachment is

(51) Hush, N. S.; Cheung, A. S. *Chem. Phys. Lett.* **1975**, *34*, 11−13.
(52) Orlov, V. N.; Smirnov, A. N.; Varshavsky, Y. M. *Tetrahedron Lett.* **1976**, *48*, 4377−4378.
(53) Richardson, N. A.; Gu, J.; Wang, S.; Xie, Y.; Schaeffer, H. F., III. *J. Am. Chem. Soc.* **2004**, *126*, 4404−4411.
(54) Weber, J. M.; Ioffe, I. N.; Berndt, K. M.; Loffler, D.; Friedrich, J.; Ehrler, O. T.; Danell, A. S.; Parks, J. H.; Kappes, M. M. *J. Am. Chem. Soc.* **2004**, *126*, 8585−8589.
(55) Dreuw, A.; Cederbaum, L. S. *Chem. Rev.* **2002**, *102*, 181−200.
(56) Simons, J. Anions. In *Encyclopedia of Mass Spectrometry Volume 1: Theory and Ion Chemistry*, 1st ed.; Armentrout, P. B., Ed.; Elsevier: 2003; pp 55−68.
(57) Emanuele, E.; Zakrzewska, K.; Markovitsi, D.; Lavery, R.; Millie, P. *J. Phys. Chem. B* **2005**, *109*, 16109−16118.

a fast process initiated by the electronic states attained by the 260-nm photons. Vibrational excitation of the ions would lead to neutral base loss or backbone fragmentation on the 50−500-ms time scale used in our ion trap experiments but would never lead to electron detachment. It can therefore be concluded that adding 4.77 eV to the closed-shell ions in electronic excited states corresponding to base excitation does not produce the same effect as adding 4.77 eV to the closed-shell ions in their vibrational modes. The nature of the excited states and how they can promote electron detachment will therefore be briefly discussed in the next section.

It is a reasonable assumption that the magnitude of the repulsive Coulomb barrier can be state-dependent because the excited states FC and E can differ by their electronic distribution. For example, state E can involve charge disproportionation (formation of a positive hole on one base and delocalization of an electron). Another possibility that was often mentioned as a possible decay mechanism of excited DNA bases is the conversion of the $\pi\pi^*$-like FC state into a $\pi\sigma^*$-like state,[1,5,58] which has a Rydberg character[1,2] (electron density away from the base). Clearly, the mechanisms by which DNA base excitation stimulates electron detachment need further investigation, and addressing excited-state dynamics in gas-phase DNA multiply charged anions is certainly a challenge for the future.

Electron photodetachment experiments like those presented here can, however, give valuable clues to get some insight in these mechanisms. In particular, the base dependence of the electron photodetachment yield brings important information. A first possible explanation involves tunneling through the repulsive Coulomb barrier (Figure 5b). Such electron tunneling through RCB has been reported previously for linear dicarboxylate dianions.[59] The tunneling probability depends on the width of the barrier, and therefore on the electron binding energy (BE), which is related to the stability of the radical. The correlation with the base IP would therefore imply that the radical in $[DNA]^{(n-1)-\bullet}$ is localized on a base (positive hole) and not on a phosphate (neutral phosphate P−O•). A second possible explanation of the base dependence involves internal coupling of the FC state to an electronic excited state characterized by the formation of a positive hole on a base and electron autodetachment from this state (Figure 5b). The efficiency of this internal coupling would then be correlated with the stability of a positive hole on a base and therefore with base IP. To decide which explanation is to be preferred, further experiments are planned with strands incorporating modified bases and other chromophores having various charge donor and charge acceptor properties.

To refine the photodetachment mechanism and the excited-state dynamics, more information is also needed on the time scale of electron photodetachment. The time scale also has important consequences on the potential application of electron photodetachment for performing spectroscopy experiments. Electron detachment channels are advantageous for spectroscopy compared to fragmentation channels because few peaks are observed in the mass spectrum and, hence, a better sensitivity. If direct electron ejection in the continuum from the FC state were the dominant process, electron photodetachment efficiency would not be wavelength-dependent as long as $h\nu > BE + RCB$. We measured the wavelength dependence of electron photodetachment yield for the strand with the lowest BE, that is, $[dG_6]^{3-}$. The results in Figure 6 shows that electron photodetachment is more efficient in the wavelength range where DNA bases are supposed to absorb, that is, around 260−270 nm. The involved excited states are therefore sufficiently long-lived to perform spectroscopy. Experiments with higher charge densities (lower RCB) are planned to explore whether direct electron ejection in the continuum could possibly occur in some cases. Furthermore, higher-resolution spectroscopy experiments on cooled ions and time-resolved measurements are planned to characterize the excited-state lifetimes.

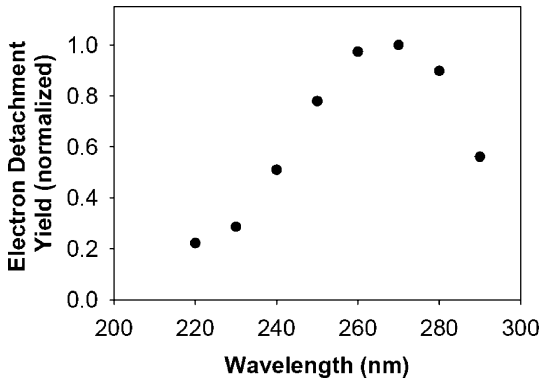

Figure 6. Relative electron photodetachment yield as a function of the wavelength for $[dG_6]^{3-}$. Electron photodetachment yield was first normalized by the laser fluence and the photon energy and then was normalized to unity.

Theoretical Calculations on Dinucleotide Monophosphates. We also took first steps in the theoretical modeling of longer DNA strands by studying dinucleotide monophosphates. As we observed that the detachment yield strongly depends on the DNA sequence, and in particular on the energy difference between the closed-shell multianion and the corresponding radical, we calculated the vertical detachment energies for several dinucleotides and also examined the highest occupied molecular orbitals (HOMO of the dBB^- and SOMO of the $dBB^\bullet$). We carried out theoretical calculations of the vertical detachment energies (VDEs) of deprotonated dinucleotide monophosphates, first using semiempirical AM1 level for a Monte Carlo conformational search, then at the HF 6-31G+(d, p) level for geometry optimization of significantly different low-energy conformers, and finally including a single-point MP2 correction for the electronic energy calculations of the anion and the neutral radical. Computation of the vertical detachment energies (VDEs) of full DNA strands such as those studied here are currently out of range (1) because vertical detachment energy is an intensive quantity while the total energy is an extensive quantity[60] and (2) because as electron correlation is already crucial in calculating the IPs of isolated DNA bases,[61] it can certainly not be neglected in the case of full DNA strands, where bases interact with one another.

The HOMOs and VDEs are shown in Figure 7 for several conformers of dGG^-, dAA^-, dCG^-, and dGT^-. The HOMO-1−HOMO-4 orbitals of these deprotonated dinucleotides are shown in Supporting Information Figures S1−S4, respectively,

(58) Sobolewski, A. L.; Domcke, W.; Dedonder-Lardeux, C.; Jouvet, C. *Phys. Chem. Chem. Phys.* **2002**, *4*, 1093−1100.
(59) Wang, L. S.; Ding, C. F.; Wang, X. B.; Nicholas, J. B.; Nicholas, B. *Phys. Rev. Lett.* **1998**, *81*, 2667−2670.
(60) Simons, J. *Adv. Quantum Chem.* **2005**, *50*, 213−233.
(61) Cauet, E.; Dehareng, D.; Lievin, J. *J. Phys. Chem. A* **2006**, *110*, 9200−9211.

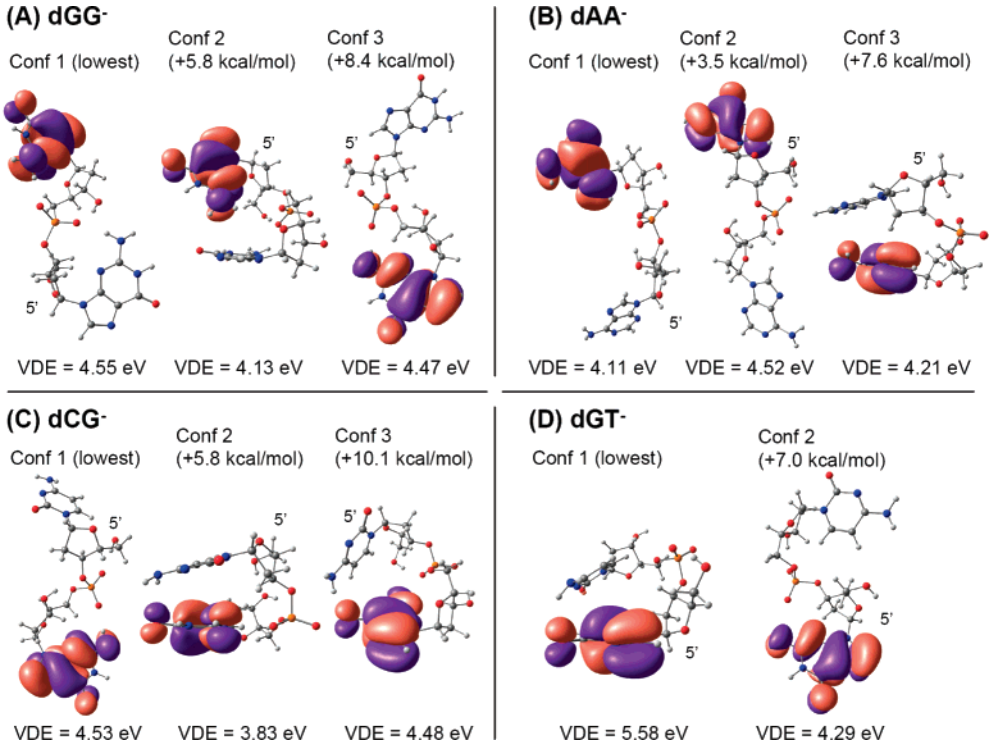

Figure 7. Relative energies (HF 6-31G+(d, p) + MP2 correction), HOMOs (HF 6-31G+(d, p)), and VDEs (HF 6-31G+(d, p) + MP2 correction) of different conformers of the deprotonated dinucleotides monophosphates (A) dGG^-, (B) dAA^-, (C) dCG^-, and (D) dGT^-.

and the SOMO of the neutral radicals are shown in Figure S5. The lowest energy conformers for dGG^-, dAA^-, and dCG^- are open, while a stacked conformer is the most stable for dGT^-, in agreement with Gidden and co-workers.[62,63] Three lessons can be learned from these calculations:

(1) The HOMO and HOMO-1 are always localized on the bases, as well as the SOMO. When the strand contains only one guanine, the HOMO and SOMO are always localized on this guanine. For the strand dGG, depending on the conformer, the SOMO can be on the other base compared to the HOMO. For the strand dAA, for all three conformers the SOMO is on the other base than the HOMO. Lowest-energy excitations therefore most likely involve the bases rather than the phosphates.

(2) Even though the energies were calculated at the MP2 level, the discrepancies between our calculations and the experimental values[46] indicate that the computation level is still not high enough. Comparison between MP2 and HF values of the VDEs (provided as Supporting Information Table S1) indicates that taking into account electron correlation significantly changes VDE, lowering it in nearly all cases.

(3) The VDEs are highly conformation-dependent. Taken together with the previous point, this suggests that geometry optimization too should take electron correlation into account, which makes accurate VDE calculation on polynucleotides really challenging. Our experiments have shown that the photodetachment yield is base-dependent and that this base dependence is correlated with the base IP. An important task in the future will be to investigate if this is a base-to-base effect or a collective effect that would be conformation-dependent. In solution, it has been suggested that hydrogen bonding, and especially base stacking, lowers the base IP,[64−67] with the consequence of a significant one-photon component in the photo-oxidation of DNA strands in aqueous solution upon 266-nm irradiation.[68−70] In particular, it has been shown that the IP of guanines was lowered in the interior of guanine runs.[66] Comparison between solution and gas-phase electron photodetachment efficiencies for different DNA structures and the study of the influence of conformation (base stacking or hydrogen bonding) on the electron binding energies of whole DNA strands will therefore help clarify the DNA photo-oxidation mechanisms.

Comparison between Electron Photodetachment, Thermal Autodetachment, and Electron Detachment Dissociation (EDD). Apart from the photodetachment method discussed here, there are two other ways of detaching electrons from DNA multiply charged ions: thermal autodetachment,[71] which is obtained when storing the DNA^{n-} into a heated ion trap for seconds to minutes, and the interaction of the DNA^{n-} with electrons having a kinetic energy of 15−18 eV,[72−74] a method known as "electron detachment dissociation", or EDD. In this

(62) Gidden, J.; Bushnell, J. E.; Bowers, M. T. *J. Am. Chem. Soc.* **2001**, *123*, 5610−5611.
(63) Gidden, J.; Bowers, M. T. *Eur. Phys. J. D* **2002**, *20*, 409−419.
(64) Sugiyama, H.; Saito, I. *J. Am. Chem. Soc.* **1996**, *118*, 7063−7068.
(65) Kim, N. S.; Zhu, Q. Q.; LeBreton, P. R. *J. Am. Chem. Soc.* **1999**, *121*, 11516−11530.
(66) Zhu, Q. Q.; LeBreton, P. R. *J. Am. Chem. Soc.* **2000**, *122*, 12824−12834.
(67) Starikov, E. B.; Lewis, J. P.; Sankey, O. F. *Int. J. Mod. Phys. B* **2005**, *19*, 4331−4357.
(68) Crespo-Hernandez, C. E.; Arce, R. *Photochem. Photobiol.* **2002**, *76*, 259−267.
(69) Crespo-Hernandez, C. E.; Arce, R. *J. Phys. Chem. B* **2003**, *107*, 1062−1070.
(70) Marguet, S.; Markovitsi, D.; Talbot, F. *J. Phys. Chem. B* **2006**, *110*, 11037−11039.
(71) Danell, A. S.; Parks, J. H. *J. Am. Soc. Mass Spectrom.* **2003**, *14*, 1330−1339.
(72) Yang, J.; Mo, J. J.; Adamson, J. T.; Hakansson, K. *Anal. Chem.* **2005**, *77*, 1876−1882.
(73) Mo, J.; Hakansson, K. *Anal. Bioanal. Chem.* **2006**, *386*, 675−681.
(74) Yang, J.; Hakansson, K. *J. Am. Soc. Mass Spectrom.* **2006**, *17*, 1369−1375.

section, we would like to highlight the similarities and differences between photodetachment and these two other methods.

The most striking difference between photodetachment and thermal detachment is the time scale. Thermal electron detachment time constants were about 1−1000 s for dB_7 (3- → 2-) for various base sequences between 100 and 150 °C. Anusiewicz et al.[75] proposed that this electron autodetachment from the ground state could be due to geometrical fluctuations of the oligonucleotide causing fluctuations in the Coulomb potential at a phosphate site of sufficient magnitude (estimated as 5 eV, which is the electron binding energy of $H_2PO_4^-$) so that the electron can tunnel through the Coulomb barrier, the rate-limiting step being the rate at which geometrical fluctuations bring the oligonucleotide in a favorable conformation for electron autodetachment. The computed electron autodetachment rate of dT_5^{3-} was 0.02−0.5 s^{-1} at $T = 170$ °C. The comparatively very short time scale characterizing electron photodetachment from DNA polyanions under 260-nm laser irradiation is a major difference. In terms of base dependence, however, there are similarities between photodetachment and thermal detachment. Danell and co-workers observed that adenine-containing strands show more efficient electron detachment than thymine-containing strands.[54,71] The base dependence was attributed to differences in oligonucleotide conformational dynamics,[54,71,75] although the authors did not completely exclude electron detachment from the bases.[54] Thermal autodetachment from guanine-containing strands was unfortunately not reported. We have seen that the base dependence can help elucidate the mechanisms of thermal detachment as well.

In electron detachment dissociation (EDD), however, no base dependence of electron detachment efficiencies was found when comparing $[dG_6]^{2-}$, $[dA_6]^{2-}$, $[dC_6]^{2-}$, and $[dT_6]^{2-}$.[74] The EDD and electron photodetachment mechanisms are therefore different. A possible explanation is that the first step in electron photodetachment involves a base excitation, which triggers electron detachment, while the electron could depart directly from a phosphate in EDD. On an analytical point of view, EDD and photodetachment are complementary, as photodetachment is more efficient than EDD for guanine-containing strands, while EDD should be preferred for non-guanine-containing strands.

Conclusions

The major findings and implications of the present work on laser irradiation of DNA multiply charged anions with 260-nm (4.77 eV) photons are as follows.

(1) Two detectable competing pathways following 260-nm photon absorption are internal conversion of electronic energy into vibrational energy, which is responsible for formation of a-base and w fragments, and electron detachment, which is detected by the charge-state change. Radiative decay could occur as well but cannot be detected with our experimental setup.

(2) Electron photodetachment is a one-photon process at 260 nm (4.77 eV).

(3) The fact that electron photodetachment can compete with excited-state relaxation by internal conversion or radiative decay suggests that electron detachment must proceed on a short time scale. This contrasts with thermal electron autodetachment from the ground state, which proceeds on time scales from seconds to minutes.

(4) The yield of electron photodetachment is base-dependent and increases as the ionization potential (IP) of the base decreases. An increased hole stability therefore increases the probability that electron detachment effectively competes with the other relaxation channels.

(5) This suggests either that electron detachment from the excited state proceeds via tunneling through the repulsive Coulomb barrier, so the tunneling efficiency is related to the stability of the product, or that electron detachment proceeds via an excited state itself involving a positive hole at a base.

(6) The yield of electron photodetachment is wavelength-dependent, with a maximum efficiency in the wavelength range presumably corresponding to DNA base absorption (260−270 nm). Calculations show that the HOMOs of deprotonated dinucleotides and SOMOs of the corresponding neutral radicals are located on the bases. Altogether, this suggests a mechanism where base excitation triggers electron detachment.

(7) Electron photodetachment can be used as a convenient channel to perform gas-phase spectroscopy studies of nucleic acids and possibly other biomolecule anions. The approach has been applied already to gas-phase spectroscopy studies of multiply charged transition-metal complexes[76,77] and polypeptides anions.[78] Future work will be devoted to the study of nucleic acid higher-order structures and complexes with DNA ligands. We recently found similar electron photodetachment channels for other chromophores bound to DNA strands (Gabelica et al., manuscript in preparation).

Acknowledgment. The GDR 2758 CNRS ≪Agrégation, fragmentation et thermodynamique des systèmes complexes isolés≫ is gratefully acknowledged for financial support. V. G. is an FNRS research associate and F. R. is an FNRS postdoctoral fellow (Fonds National de la Recherche Scientifique, Belgium). HP Belgium is gratefully acknowledged for the loan of two linux HP ProLiant ML570 G3 demonstration servers.

Supporting Information Available: Table S1 (comparison of VDEs at Koopmans, HF, and MP2 level) and Figures S1−S4 (HOMO to HOMO-4 of all dinucleotide models) and Figure S5 (SOMO of the dinucleotide radicals) are provided as Supporting Information. This material is available free of charge via the Internet at http://pubs.acs.org.

JA068440Z

(75) Anusiewicz, W.; Berdys-Kochanska, J.; Czaplewski, C.; Sobczyk, M.; Daranowski, E. M.; Skurski, P.; Simons, J. *J. Phys. Chem. A* **2005**, *109*, 240−249.

(76) Kordel, M.; Schooss, D.; Gilb, S.; Blom, M. N.; Hampe, O.; Kappes, M. M. *J. Phys. Chem. A* **2004**, *108*, 4830−4837.

(77) Loffler, D.; Weber, J. M.; Kappes, M. M. *J. Chem. Phys.* **2005**, *123*, 224308.

(78) Antoine, R.; Joly, L.; Tabarin, T.; Broyer, M.; Dugourd, P.; Lemoine, J. *Rapid Commun. Mass Spectrom.* **2007**, *21*, 265−268.